Research Square

Preprints are preliminary reports that have not undergone peer review.
They should not be considered conclusive, used to inform clinical practice,
or referenced by the media as validated information.

Integrative morphological and multilocus molecular analysis reveals intraspecific genetic structuring in Anoectochilus roxburghii (Orchidaceae) from central Vietnam

Nhi Thi Hoang Ho
hothihoangnhi@hueuni.edu.vn
Institute of Biotechnology
Han Ngoc Ho
Institute of Biotechnology
Hai Thi Hong Truong
Institute of Biotechnology

Research Article

Keywords: Anoectochilus roxburghii, DNA barcoding, genetic diversity, ITS, SSR markers, species conservation

Posted Date: March 13th, 2026

DOI: https://doi.org/10.21203/rs.3.rs-9016426/v1

License: This work is licensed under a Creative Commons Attribution 4.0 International License.
Read Full License

Additional Declarations: No competing interests reported.

Integrative morphological and multilocus molecular analysis reveals intraspecific genetic structuring in *Anoectochilus roxburghii* (Orchidaceae) from central Vietnam

NHI THI HOANG HO [1]*, HAN NGOC HO[1], HAI THI HONG TRUONG[1]*
[1]Institute of Biotechnology, Hue University, Hue city 53000, Vietnam,
*Corresponding author: Nhi Thi Hoang Ho (email: hothihoangnhi@hueuni.edu.vn) and Hai Thi Hong Truong (email: tthhai@hueuni.edu.vn)

Abstract: *Anoectochilus* is a high-value medicinal orchid threatened by overexploitation and habitat degradation. However, integrated micro-morphological and molecular data for natural Vietnamese populations remain limited. This study provided a comprehensive characterisation of 17 accessions collected from Bach Ma National Park using detailed micro-anatomical analysis, multi-locus DNA barcoding (*ITS*, *rbcL*, *psbA-trnH*), and SSR-based genetic profiling. Micro-morphological assessment revealed substantial intra-population differences. Additionally, correlations between anatomical traits and vegetative growth parameters suggested structural contributions to phenotypic variability. DNA barcoding confirmed species identity, *Anoectochilus roxburghii*, with high similarity (98.92–100%) to reference sequences. Among the tested barcode loci, ITS exhibited the highest discriminatory power. Despite low nucleotide diversity in barcode regions, SSR analysis detected moderate-to-high polymorphism (He ≥ 0.408; PIC ≥ 0.327) and resolved the population into four genetic clusters with similarity coefficients ranging from 0.39 to 0.93. This contrast between barcode homogeneity and SSR diversity showed the evolutionary process within the population. Moreover, these findings could establish a good baseline for conservation management and future marker-assisted breeding of *A. roxburghii*.

Keywords: *Anoectochilus roxburghii*; DNA barcoding; genetic diversity; ITS; SSR markers; species conservation

Running title: Integrative morphological and multilocus molecular analysis of *Anoectochilus*

INTRODUCTION

Anoectochilus roxburghii (Wall.) Lindl is a highly valuable species in many Asia contries due to its ornamental, medicinal, food and cosmetic purposes (Ye et al. 2019). It has been demonstrated to have anti-inflammatory, antioxidant, antitumor, antiviral, and antihyperlipidemic effects (Zou et al. 2025). However, it was listed as a hazardous or near-threatened species in the Convention on International Trade in Endangered Species of Wild Fauna and Flora (Wang et al. 2022) and included in the Vietnam Red Book of endangered species (Tran et al. 2022). This is due to slow growth, low natural propagation rate, specific habitat requirements, animal consumption, indiscriminate collection, and increasing human demand (Hou et al. 2025; Zhang et al. 2013). Therefore, conservation activities for this species need to be carried out. Genetic and morphological information is essential in this activity. Conservation genetics is fundamental to conservation biology, as it assesses genetic variation and the future survival potential of a species (Woodruff 2001). Meanwhile, morphology (external form) and anatomy (internal tissue structure) are used to classify, describe, and identify plant species (Barwant et al. 2024). By combining both methods, studies can achieve higher taxonomic resolution, more precise species delineation, and a broader understanding of evolutionary relationships and biodiversity (Zaman et al. 2025).

Morphological studies in *Anoectochilus* primarily focus on characteristics such as leaves, stems, flowers, and roots (Bhattacharjee 2013; Ye et al. 2017; Zhang et al. 2024), while DNA barcoding is a suitable method for molecular identification of rare endemic and endangered species (Safhi et al. 2023). Among DNA barcode markers, the internal transcribed spacer (*ITS*) is a powerful phylogenetic marker due to its widespread distribution and the greater evolutionary rate. In addition, it is a non-coding region and exhibits more variation (Letsiou et al. 2024). Hence, many studies used *ITS* for identification of *Anoectochilus* species (Gao et al. 2009; Hu et al. 2019; Lv et al. 2025; Thinh et al. 2020). In addition, *psbA-trnH* and *rbcL* (ribulose bisphosphate carboxylase/oxygenase large subunit) regions were also analysed to evaluate genetic differences between *Anoectochilus* accessions (Ho et al. 2021; Lv et al. 2015; Wang et al. 2025). *psbA-trnH* is one of the most variable non-coding plastid loci, exhibiting a large level of species discrimination and high rates of insertion/deletion (Letsiou et al. 2024). Meanwhile, the *rbcL* region had a greater distinguishing potential than the *matK* (maturase K) region (Ho et al. 2021). Moreover, simple sequence repeat (SSR) markers have many advantages, including high polymorphism, codominance, high repeatability, universality, and abundant information, for analysing genetic diversity and resource identification (Ding et al. 2025; Su et al. 2025; Zhao et al. 2023). This approach can facilitate the conservation and improvement of endangered species and guide breeding programs (Sontikun et al. 2025). Previously, Lu (2022) and Zhang et al. (2024) successfully applied SSR markers in transcriptome analysis to assess genetic and morphological diversity.

Our previous research investigated and discovered the distribution characteristics of *Anoectochilus* in Bach Ma National Park, central Vietnam (Ho et al. 2025b). However, to conserve and develop this species, scientific data on morphology and molecular and genetic differences within the population need to be analysed. To address this purpose, we conducted (1) collection and analysis of morphological and microphonic characteristics, (2) molecular identification based on DNA barcode sequences (*ITS*, *rbcL* and *psbA-trnH*), and (3) examination of genetic diversity among accessions using SSR markers.

MATERIALS AND METHODS

Plant materials

Seventeen *Anoectochilus* accessions were utilised in this study (Table 1). These accessions were collected from Bach Ma National Park, central Vietnam in 2024 (Ho et al. 2025b). They were then cultured in the laboratory conditions at a temperature of 25 - 26 °C, humidity of 70 - 80% and light intensity of 2000 lux.

Table 1 List of *Anoectochilus* accessions used in this study.

S. N.	Accession	Code	Coordinates	Place of collection
1	HUIB_AR1	AR1	16°11'36.2"N; 107°50'56.5"E	Loc Tri, Phu Loc, Hue city
2	HUIB_AR2	AR2	16°13'45.4"N; 107°50'53.2"E	Loc Tri, Phu Loc, Hue city
3	HUIB_AR3	AR3	16°11'29.4"N; 107°44'26.1"E	Huong Phu, Huong Thuy, Hue city
4	HUIB_AR4	AR4	16°11'26.7"N; 107°45'04.1"E	Huong Phu, Huong Thuy, Hue city
5	HUIB_AR5	AR5	16°11'09.4"N; 107°45'21.5"E	Huong Phu, Huong Thuy, Hue city
6	HUIB_AR6	AR6	16°11'08.1"N; 107°45'26.4"E	Huong Phu, Huong Thuy, Hue city
7	HUIB_AR7	AR7	16°04'58.1"N; 107°45'02.4"E	Thuong Lo, Dong Giang, Hue city
8	HUIB_AR8	AR8	16°04'45.9"N; 107°45'23.2"E	Thuong Lo, Dong Giang, Hue city
9	HUIB_AR9	AR9	16°08'12.4"N; 107°50'49.0"E	Thuong Lo, Dong Giang, Hue city
10	HUIB_AR10	AR10	16°07'55.4"N; 107°51'09.0"E	Thuong Lo, Dong Giang, Hue city
11	HUIB_AR11	AR11	16°07'54.2"N; 107°51'12.3"E	Thuong Lo, Dong Giang, Hue city
12	HUIB_AR12	AR12	16°07'53.1"N; 107°51'26.4"E	Thuong Lo, Dong Giang, Hue city
13	HUIB_AR13	AR13	16°11'34.5"N; 107°50'44.2"E	Loc Dien, Phu Loc, Hue city
14	HUIB_AR14	AR14	16°07'27.9"N; 107°47'16.4"E	Thuong Lo, Dong Giang, Hue city
15	HUIB_AR15	AR15	16°13'04.1"N; 107°43'53.6"E	Huong Phu, Huong Thuy, Hue city
16	HUIB_AR16	AR16	16°13'03.9"N; 107°44'50.9"E	Huong Phu, Huong Thuy, Hue city
17	HUIB_AR17	AR17	16°12'06.5"N; 107°44'50.6"E	Huong Phu, Huong Thuy, Hue city

Micro-morphological identification

Morphological identification

Quantitative morphological traits included stem length (SL), number of stem nodes (NSN), stem node length (NL), number of leaves (NOL), leaf length (LL), leaf width (LW), number of main veins (NV), petiole diameter (PD) and petiole length (PL). Qualitative morphological traits included plant habit (PH), plant growth (PG), kinds of stem (KS), stem color (SC), texture of stem (TS), vein color on the leaf's upper surface (VUP), vein color on the leaf's lower surface (VUD), mesophyll color on the leaf's upper surface (MUP), mesophyll color on the leaf's under surface (MUD), leaf shape (LSH), leaf surface (LSF), leaf margin (LM), petiole color (PC), leaf sheath color (LSC), root color (RC) and root habit (RH). These traits were scored at the full foliage stage at one months post transplanting.

Microphonic identification

Accessions were prepared for microscopic imaging based on the method of Truong et al. (2025). Sixteen microphonic traits were studied including number of epidermal cell layers of stem (NEPS), number of collenchyma cell layers of stem (NCS), number of parenchyma cell layers of stem (NPS), number of edodermal cell layers of stem (NEDS), number of xylem bundles of stem (NXS), number of phloem bundles of stem (NPHS), Number of pith cell layers of stem (NPIS), number of epidermal cell layers of petiole (NEPP), number of collenchyma cell layers of petiole (NCP), number of parenchyma cell layers of petiole (NPP), number of xylem bundles of stem (NXP), number of phloem bundles of stem (NPHP), number of upper epidermal cell layers of leaf (NUEL), number of lower epidermal cell layers of leaf (NLEL), number of palisade mesophyll cell layers (NPM) and number of spongy mesophyll cell layers (NSM). Furthermore, quantitative traits were then compiled to evalution correlation among them. PAST v4.03 software was used in this analysis.

DNA extraction, PCR and DNA barcoding

Genomic DNA was extracted from adult leaves of each accession by the CTAB method (cetyl trimethyl ammonium bromide) and purified (Ho et al. 2025a). Next, they were amplified with *ITS*, *psbA-trnH* and *matK* primers in a PCR system (Applied Biosystems, USA) (Table 2). Each 20 µL PCR contained 50 ng DNA, 10 µL of 2X MyTaq Mix (Meridian Bioscience, US) and 1 µM of primer. The thermocycling program was described in Table 2. PCR products were then sequenced in 1st BASE (Apical Scientific Sdn. Bhd., Malaysia) and analysed with BLASTn available on the NCBI. Used parameters in BLASTn included >97% identity, 0.0 e-value and >85% coverage. Next, a phylogenetic tree was constructed in MEGA 12 software (Kumar et al. 2024) based on the Neighbor-Joining method with a Kimura 2-parameter model and 1000 bootstrap replicates. The sequencing data in this work were aligned with some reference sequences of *Anoectochilus* species that downloaded from BOLD (https://www.boldsystems.org/). Besides, DnaSP v6 software was applied to evaluate parameters of sequence, including the number of variable (polymorphic) sites, the number of mutations, nucleotide diversity, average number of nucleotide differences, number of Haplotypes and Haplotype diversity (Rozas et al. 2017).

SSR markers

The SSR analysis was carried out in 10 µL PCR containing 30 ng of DNA, 5 µL of 2x MyTaq buffer and 0.5 µM SSR primers (Table 2). The PCR products were then stained with SYBR Green, separated on 3% agarose gel (0.5X TBE buffer) and observed under UV light. DNA bands of the same size represented the same allele. The scored data of bands were analysed using NTSYSpc 2.1 to determine the genetic distance among accessions and construct the UPGMA dendrogram. The number of alleles was used to calculate successful amplification rate, band size, observed number of alleles (na), effective number of alleles (ne), Shannon's Information index (I), polymorphism information content (PIC),

expected heterozygosity (He) and observed heterozygosity (Ho) using POPGENE 1.32 and Cervus 3.0.7 (Kalinowski et al. 2007).

Table 2 List of DNA barcode primers and SSR primers.

Primer name		Forward sequence (5′–3′)	Reverse sequence (5′–3′)	PCR conditions	Reference
DNA barcode primers	*ITS*	AGGAGAAGTCGTAACAAGGTTTCC	GATATGCTTAAACTCAGCGGGTC	94 °C (4 min); 30 cycles- 94 °C (30 s), 55 °C (40 s), 72 °C (40 s); 72 °C (5 min)	Thinh et al. 2020
	psbA-trnH	GTTATGCATGAACGTAATGCTC	CGCGCATGGTGGATTCACAATCC	95 °C (2 min); 35 cycles- 95 °C (30 s), 53.8 °C (30 s), 72 °C (1 min); 72 °C (5 min)	Lv et al. 2015
	rbcL	TGAAAACGTGAATTCCCAACCGTTTATGCG	GCAGCAGCTAGTTCCGGGCTCCA	95 °C (2 min); 35 cycles- 95 °C (30 s), 55 °C (30 s), 72 °C (1 min); 72 °C (5 min)	Ho et al. 2021
SSR primers	3-4FR	CCGGATCCAGCAAACACTCT	GCCGCCGTCTATTGGTAGAA	95 °C (3 min); 35 cycles- 95 °C (40 s), 60 °C (30 s), 72 °C (1 min); 72 °C (8 min)	Zhang et al. 2024
	2-5FR	AGGAGGCGTTCGTGAAGAAG	GTATCATCAGAGCCGCCCAA	95 °C (3 min); 35 cycles- 95 °C (40 s), 59 °C (30 s), 72 °C (1 min); 72 °C (8 min)	
	3-2FR	GCAGCTTTTGTCGCAGCTAT	TGGAAGCTTGGGTAACAACAGA		
	3-9FR	AGAGGATGGTGCCAATGTTGT	GAGCATCGTTTTCATCGCCC		
	4-1FR	GAGAGAGCTTCCGACGATGG	TTCCCCAACAGGAATCCTCG		
	4-3FR	CTCTCCACCTCTCTCCCTCC	TCTTTCACAGCCATCGCAGT		

RESULTS

Micro-morphological characterisation

In terms of morphological characteristics, all *Anoectochilus* accessions grew erect; the stem structure was hard; the leaf veins were glitter on the upper surface and light green on the lower surface; the mesophyll on the leaf upper surface was dark green; the leaves were orbicular, smooth, and had sinusoidal margins; the petioles were green; the roots were creeping and brownish-green. The growth of the samples was uneven, with most samples growing moderately to well. Only HUIB_AR6, HUIB_AR8, and HUIB_AR13 showed weak growth due to fungal infection causing root and leaf rot (Fig. 1). The purplish-green color of HUIB_AR10 stem was distinctly different from the green stems of the other samples. Meanwhile, the purplish-green color of the lower leaf mesophyll only appeared in HUIB_AR2 and HUIB_AR15. The green color of the leaf sheath was only present in HUIB_AR3 and HUIB_AR9 (Table 3, Fig. 1).

Quantitative morphological traits were collected; however, the collected data were insufficient for a statistical biological assessment due to the rarity of this species. Overall, there was considerable variation in these traits. The average stem length was 8.22 cm, with sample HUIB_AR7 having the greatest length (15.5 cm). The number of stem nodes and leaves varied greatly among accessions, ranging from 2 to 7. HUIB_AR2 and HUIB_AR7 had the longest node lengths, at 2.02 and 2.03 nodes/plant, respectively. The largest leaf size was observed in HUIB_AR4 and HUIB_AR14. On average, there were 5.31 main veins per leaf, with the highest number of veins (7 veins) observed in HUIB_AR5. Additionally, most accessions had petiole diameters exceeding 0.2 cm and petiole lengths exceeding 0.6 cm. Notably, HUIB_AR14 and HUIB_AR15 had the largest number of xylem and phloem bundles (22 and 20 bundles/stem, respectively). This may indicate the best growth potential of these two accessions. HUIB_AR11 had a thicker petiole than the other samples with the most parenchyma layers (12 layers). Furthermore, the leaf cross-section of sample HUIB_AR16 was different from the others, showing 10 cell layers, including one upper epidermis, one lower epidermis, three palisade cell layers, and five spongy mesophyll cell layers (Table 4, Fig. 2).

Based on the results of correlation analysis between quantitative traits, changes in stem length and stem node size were significantly correlated with changes in leaf and petiole size. This change was due to an increase in the number of parenchyma cell layers, pith cell layers, and xylem and phloem vascular bundles in plant parts. Meanwhile, the number of veins per leaf appeared to be inversely proportional to petiole length, the number of xylem bundles and phloem bundles, and the number of pith cell layers in the stem (Fig. 3).

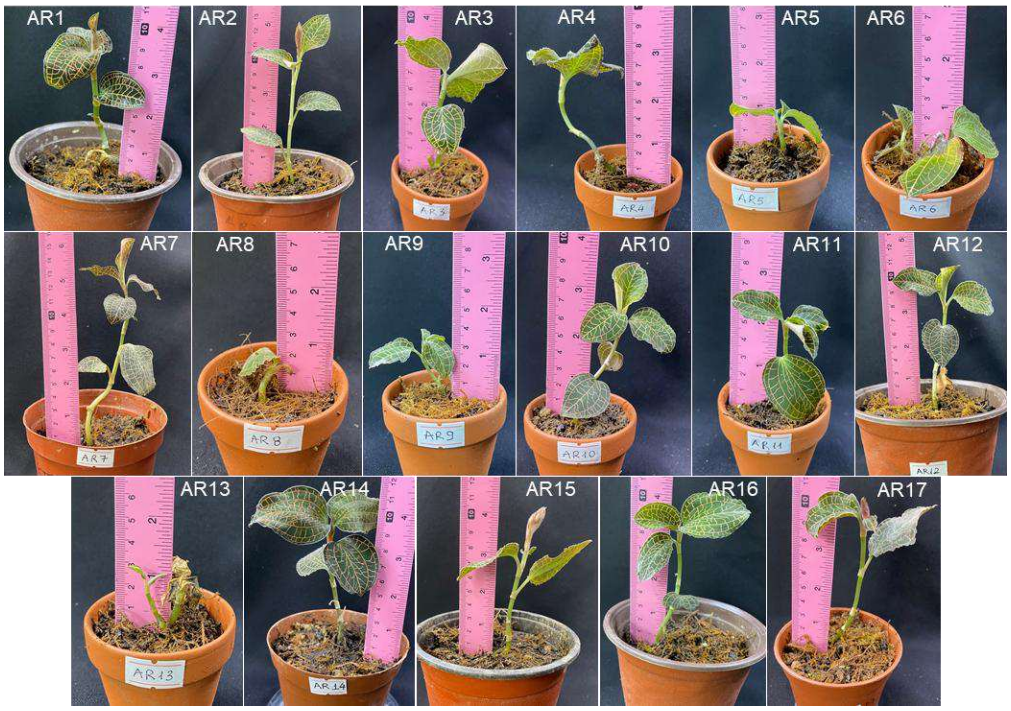


Fig. 1 Morphology of 17 *Anoectochilus* accessions in this study.

Table 3 Qualitative morphological traits observed in *Anoectochilus* accessions.

Accessions	PH	PG	PG	SC	TS	VUP	VUD	MUP	MUD	LSH	LSF	LM	PC	LSC	RC	RH
AR1	1	3	1	1	1	1	1	1	1	1	1	1	1	2	1	1
AR2	1	3	1	1	1	1	1	1	2	1	1	1	1	2	1	1
AR3	1	3	1	1	1	1	1	1	1	1	1	1	1	1	1	1
AR4	1	3	1	1	1	1	1	1	1	1	1	1	1	2	1	1
AR5	1	2	1	1	1	1	1	1	1	1	1	1	1	2	1	1
AR6	1	1	1	1	1	1	1	1	1	1	1	1	1	2	1	1
AR7	1	3	1	1	1	1	1	1	1	1	1	1	1	2	1	1
AR8	1	1	1	1	1	1	1	1	1	1	1	1	1	2	1	1
AR9	1	2	1	1	1	1	1	1	1	1	1	1	1	1	1	1
AR10	1	3	1	2	1	1	1	1	1	1	1	1	1	2	1	1
AR11	1	3	1	1	1	1	1	1	1	1	1	1	1	2	1	1
AR12	1	3	1	1	1	1	1	1	1	1	1	1	1	2	1	1
AR13	1	1	1	1	1	1	1	1	1	1	1	1	1	2	1	1
AR14	1	3	1	1	1	1	1	1	1	1	1	1	1	2	1	1
AR15	1	3	1	1	1	1	1	1	2	1	1	1	1	2	1	1
AR16	1	3	1	1	1	1	1	1	1	1	1	1	1	2	1	1
AR17	1	3	1	1	1	1	1	1	1	1	1	1	1	2	1	1

PH; Plant habit: Erect (1)
PG; Plant growth: Poor (1), Medium (2), Good (3).
KS; Kinds of stem: Rhizomatous (1)
SC; Stem color: Green (1), Purplish green (2)
TS; Texture of stem: Hard (1)
VUP; Vein color on the leaf's upper surface: Glitter (1)
VUD; Vein color on the leaf's lower surface: Light green (1)
MUP: Mesophyll color on the leaf's upper surface: Dark green (1)
MUD: Mesophyll color on the leaf's under surface: Purple (1), Greenish purple (2)
LSH; Leaf shape: Orbicular (1)
LSF; Leaf surface: Glabrous (1)
LM; Leaf margin: Sinuate (1)
PC; Petiole color: Green (1)
LSC; Leaf sheath color: Green (1), Purplish green (2)
RC; Root color: Greenish brown (1)
RH; Root habit: Creeping (1)

Table 4 Quantitative micro-morphological features observed in *Anoectochilus* accessions.

Accessions	**SL**	**NSN**	**NL**	**NOL**	**LL**	**LW**	**NV**	**PD**	**PL**	**NEPS**	**NCS**	**NPS**	**NEDS**
AR1	11	6	1.60	4	3.50	2.55	6.50	0.23	0.38	1	1	14	2
AR2	12	6	2.02	4	3.65	2.48	5.00	0.20	1.18	1	1	14	2
AR3	8.5	6	1.34	4	3.23	2.48	5.25	0.20	0.68	1	1	12	2
AR4	10	5	1.50	3	4.43	2.90	5.33	0.20	1.00	1	1	12	2
AR5	3.3	2	1.50	2	3.25	2.70	7.00	0.20	0.60	1	1	11	2
AR6	3	3	0.90	3	2.00	1.53	5.00	0.10	0.60	1	1	12	2
AR7	15.5	7	2.03	7	3.31	2.56	5.57	0.24	0.97	1	1	14	2
AR8	2.5	2	1.75	2	3.55	3.00	5.00	0.25	0.65	1	1	11	2
AR9	4.7	4	1.05	4	2.25	1.55	5.00	0.10	0.65	1	1	11	2

AR10	7.5	5	1.44	5	3.20	2.36	5.00	0.14	0.72	1	1	12	2
AR11	8	6	1.42	4	2.95	1.95	5.25	0.16	0.88	1	1	12	2
AR12	11	6	1.70	4	3.53	2.78	5.00	0.20	1.03	1	1	14	2
AR13	3.6	3	1.23	3	1.83	1.20	5.00	0.17	0.80	1	1	12	2
AR14	9.5	6	1.43	5	4.34	3.20	5.00	0.25	1.04	1	1	11	2
AR15	10.5	6	1.33	3	3.53	2.57	5.33	0.23	1.10	1	2	11	2
AR16	8.7	5	1.54	4	3.50	2.55	5.00	0.19	0.88	1	1	14	2
AR17	10.5	5	1.88	3	3.20	2.07	5.00	0.18	0.83	1	1	12	2
Mean	8.22	4.88	1.51	3.76	3.25	2.38	5.31	0.19	0.82	1.00	1.06	12.29	2.00
Accessions	**NXS**	**NPHS**	**NPIS**	**NEPP**	**NCP**	**NPP**	**NXP**	**NPHP**	**NUEL**	**NLEL**	**NPM**	**NSM**	
AR1	12	12	6	1	1	9	5	5	1	1	3	3	
AR2	16	16	9	1	1	7	5	5	1	1	2	3	
AR3	14	14	6	1	1	10	5	5	1	1	2	4	
AR4	17	17	6	1	1	10	5	5	1	1	2	4	
AR5	11	11	6	1	1	8	5	5	1	1	2	4	
AR6	11	11	6	1	1	8	5	5	1	1	2	4	
AR7	19	19	7	1	1	8	5	5	1	1	2	4	
AR8	12	12	6	1	1	7	5	5	1	1	2	3	
AR9	11	11	6	1	1	8	5	5	1	1	2	3	
AR10	17	17	6	1	1	8	5	5	1	1	2	3	
AR11	14	14	6	1	1	12	5	5	1	1	3	4	
AR12	12	12	6	1	1	10	5	5	1	1	3	4	
AR13	11	11	6	1	1	5	3	3	1	1	2	3	
AR14	23	23	8	1	1	8	5	5	1	1	2	5	
AR15	20	20	8	1	1	7	5	5	1	1	2	5	
AR16	16	16	9	1	1	7	5	5	1	1	3	5	
AR17	16	16	8	1	1	10	5	5	1	1	2	4	
Mean	14.82	14.82	6.76	1.00	1.00	8.35	4.88	4.88	1.00	1.00	2.24	3.82	

SL: Stem length (cm), NSN: Number of stem nodes (node/stem), NL: Stem node length (cm), NOL: Number of leaves (leaf/plant), LL: Leaf length (cm), LW: Leaf width (cm), NV: Number of main veins (vein/leaf), PD: Petiole diameter (cm), PL: Petiole length (cm), NEPS: Number of epidermal cell layers of stem, NCS: Number of collenchyma cell layers of stem, NPS: Number of parenchyma cell layers of stem, NEDS: Number of edodermal cell layers of stem, NXS: number of xylem bundles of stem, NPHS: number of phloem bundles of stem, NPIS: Number of pith cell layers of stem, NEPP: Number of epidermal cell layers of petiole, NCP: Number of collenchyma cell layers of petiole, NPP: Number of parenchyma cell layers of petiole, NXP: number of xylem bundles of stem, NPHP: number of phloem bundles of stem, NUEL: Number of upper epidermal cell layers of leaf, NLEL: Number of lower epidermal cell layers of leaf, NPM: Number of palisade mesophyll cell layers, NSM: Number of spongy mesophyll cell layers.

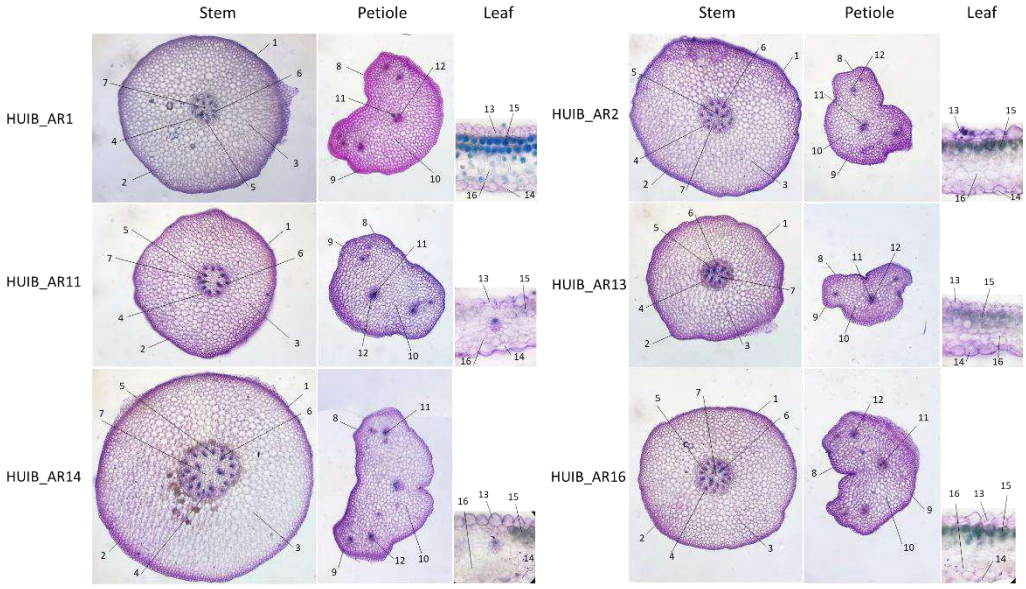


Fig. 2 Microphonic features of HUIB_AR1, HUIB_AR2, HUIB_AR11, HUIB_AR13, HUIB_AR14 and HUIB_AR16.
1. Stem epidermis, 2. Stem collenchyma, 3. Stem parenchyma, 4. Stem edodermis, 5. Stem xylem, 6. Stem phloem, 7. Stem pith, 8. Petiole epidermis, 9. Petiole collenchyma, 10. Petiole parenchyma, 11. Petiole xylem, 12. Petiole phloem, 13. Upper epidermis in leaf, 14. Lower epidermis in leaf, 15. Palisade mesophyll in leaf, 16. Spongy mesophyll in leaf.

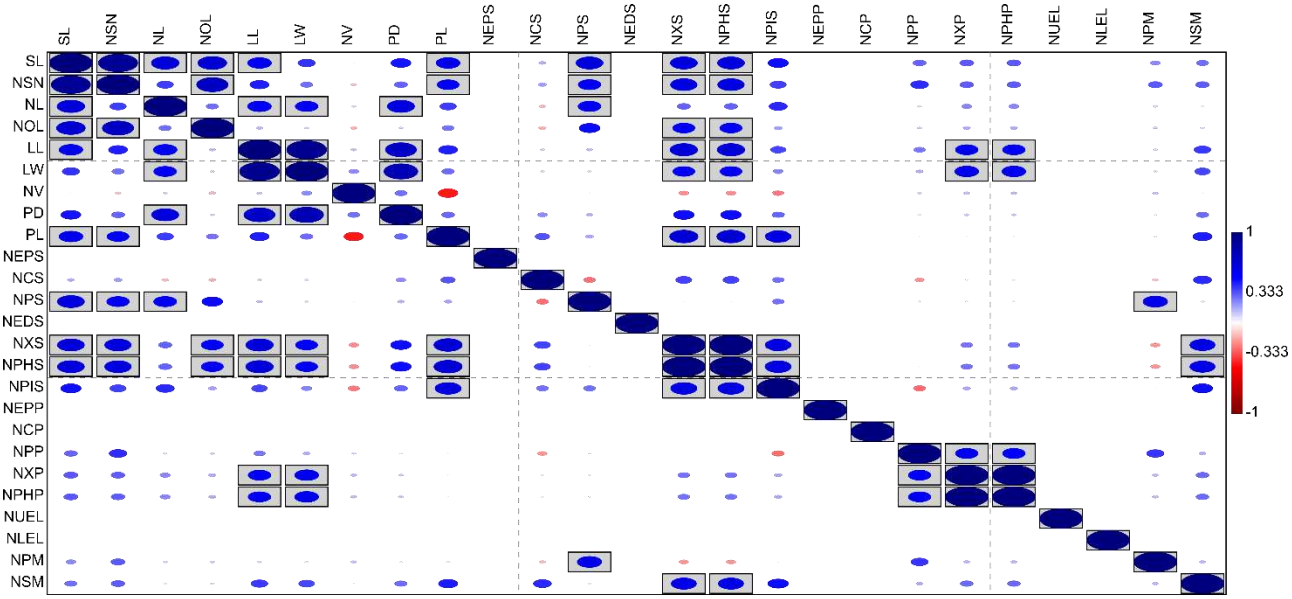


Fig. 3 Correlation among quantitative micro-morphological traits of *Anoectochilus* accessions. Squares indicate statistically significant correlations.

Analysis of *ITS*, *rbcL* and *psbA-trnH* sequences among 17 accessions

Seventeen *Anoectochilus* accessions were successfully sequenced and published on NCBI. The *ITS*, *rbcL* and *psbA-trnH* sequences were 740 bp, 731 bp long and 857 bp, respectively. Referencing these sequences in the Genbank database showed high genetic similarity (98.92-100%) to *A. roxburghii* and *A. setaceus* (synonymous with *A. roxburghii* (Wall.) Lindl.) (Table 5). Additionally, the *ITS* data in this study were compared with *ITS* sequences of seven *Anoectochilus* from the BOLD database. The phylogenetic tree divided the population into two clusters, and it also revealed the genetic relationship between 17 accessions and *A. setaceus* in 50 bootstraps (Fig. 4A). Cluster 1 included HUIB_AR4, HUIB_AR8, HUIB_AR9, HUIB_AR12, HUIB_AR13, HUIB_AR14, HUIB_AR15, and HUIB_AR16, while the remaining accessions were classified into cluster 2. These clusters were created by a single-nucleotide polymorphism in the *ITS* region. Specifically, HUIB_AR1, HUIB_AR2, HUIB_AR3, HUIB_AR5, HUIB_AR6, HUIB_AR7, HUIB_AR10, HUIB_AR11, and HUIB_AR17 had Guanine (G) at nucleotide 525, while others carried Adenine (A) at the same position (Fig. 4B).

The *rbcL* sequence in all accessions was completely identical; however, it differed from the *rbcL* sequence on GenBank (NC_061758.1). Conversely, similar to results of *ITS*, the *trnH-psbA* region showed inter-accession variability. Eight polymorphic nucleotides were found in only six accessions: HUIB_AR8, HUIB_AR9, HUIB_AR11, HUIB_AR12, HUIB_AR14 and HUIB_AR15. This was due to variations in the number of repeats of the TTAGTATA sequence (Fig. 4C). Specifically, these six accessions had (TTAGTATA)3 from nucleotide position 240, while others only had (TTAGTATA)2. However, when considering the population indices of the *psbA-trnH* and *rbcL* regions, all of them had values of 0 (Table 6).

The *ITS* region was the most promising for assessing differentiation within the *Anoectochilus* population because it reports the highest evaluation indices values. Combining DNA barcode sequences to assess relationships between accessions was not promising. The two combinations (*ITS* + *psbA-trnH* and *ITS* + *rbcL* + *psbA-trnH*) had constant S, Eta, k, h and Hd values, while π tended to decrease from 0.72 x 10^{-3} to 0.33 x 10^{-3} and 0.23 x 10^{-3} compared to results of ITS (Table 6).

Table 5 Results obtained from sequencing and referencing the DNA barcode sequences of accessions with GenBank data.

Regions	Accessions	GenBank accession number	Sequencing results			Referencing results			
			Successful sequencing rate (%)	Size (bp)	Number of variable nucleotide	Query cover (%)	e-value	Percent identity (%)	Reference sequence in GenBank
ITS	HUIB_AR1, HUIB_AR2, HUIB_AR3, HUIB_AR5, HUIB_AR6, HUIB_AR7, HUIB_AR10, HUIB_AR11 and HUIB_AR17	PV785251 – PV785267	100	740	1	100	0	99.73	KR815828.1 (*A. roxburghii*)
	HUIB_AR4, HUIB_AR8, HUIB_AR9, HUIB_AR12, HUIB_AR13, HUIB_AR14, HUIB_AR15 and HUIB_AR16		100	740	1	100	0	99.86	
rbcL	All accessions	PX899751 – PX899767	100	731	0	100	0	99.04	NC_061758.1 (*A. roxburghii*)
psbA-trnH	HUIB_AR1, HUIB_AR2, HUIB_AR3, HUIB_AR4, HUIB_AR5, HUIB_AR6, HUIB_AR7, HUIB_AR10, HUIB_AR13, HUIB_AR16 and HUIB_AR17	PX910683 – PX910699	100	857	8	86	0	100	PV330332.1 (*A. setaceus*)

Regions	Accessions	GenBank accession number	Sequencing results			Referencing results			
			Successful sequencing rate (%)	Size (bp)	Number of variable nucleotide	Query cover (%)	e-value	Percent identity (%)	Reference sequence in GenBank
	HUIB_AR8, HUIB_AR9, HUIB_AR11, HUIB_AR12, HUIB_AR14 and HUIB_AR15		100	865	8	86	0	98.92	

Table 6 Evaluation indices of *Anoectochilus* population based on of the *ITS*, *rbcL* and *psbA-trnH* region.

Indices	*ITS*	*rbcL*	*psbA-trnH*	*ITS* + *psbA-trnH*	*ITS* + *rbcL* + *psbA-trnH*
No. of variable sites, S	1	0	0	1	1
No. of mutations, Eta	1	0	0	1	1
Nucleotide diversity (per site), π ($x10^{-3}$)	0.72	0	0	0.33	0.23
Average number of nucleotide differences, k	0.52941	0	0	0.52941	0.52941
Number of haplotypes, h	2	0	0	2	2
Haplotype diversity, Hd	0.529	0	0	0.529	0.529

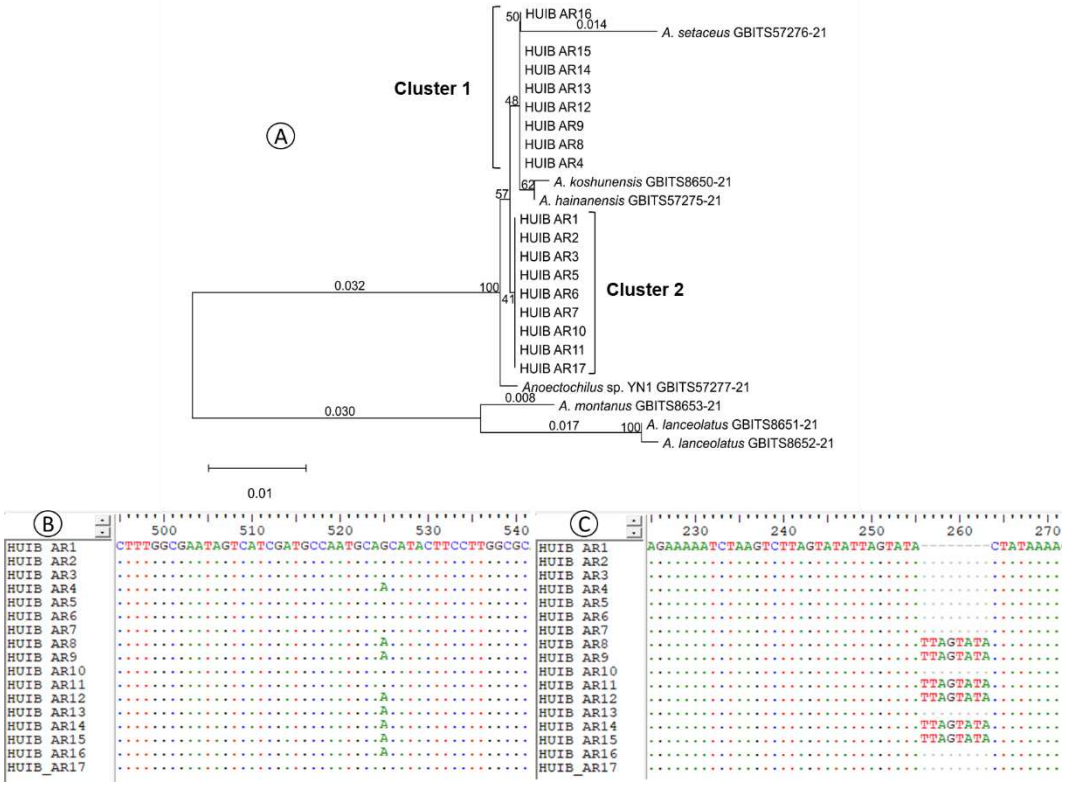


Fig. 4 The phylogenetic tree of the *ITS* region using the Neighbor-Joining method (A) and nucleotide differences between accessions in the *ITS* (B) and *psbA-trnH* region (C).

SSR analysis

Most SSR primers successfully amplified all accessions, except for the 3-2FR primer with an amplification rate of 82.35%. The generated product bands ranged in size from 170 bp to 450 bp, and there were differences in amplified band size between accessions (Fig. 5). The mean observed number of alleles (na) and mean effective number of alleles (ne) were 4.500 and 2.689, respectively. Four primers (2-5FR, 3-2FR, 3-9FR, and 4-1FR) reported the highest I and PIC values. Additionally, expected heterozygosity (He) ranged from 0.373 to 0.779, with loci having expected heterozygosity of 0.5 or higher only found in 2-5FR, 3-2FR, 3-9FR, and 4-1FR. This result differed significantly from the observed heterozygosity (Ho), particularly in primers 2-5FR, 3-4FR, and 4-1FR (Table 7). High values of I, PIC, and He indicated differences in the sequences of 17 accessions. Furthermore, the UPGMA tree generated from the SSR data divided the *Anoectochilus* population into four clusters at a coefficient of 0.7. The similarity coefficients of the accessions ranged from 0.39 to 0.93. Cluster 1 included HUIB_AR1, HUIB_AR2, and HUIB_AR7. Clusters 2 and 3 contained 8 and 5 accessions, respectively. Meanwhile, HUIB_AR15 in cluster 4 showed the most genetic separation from the others (Fig. 6).

Table 7 Genetic diversity at various loci in *Anoectochilus* accessions using six SSR primers.

Primer	Successful amplification rate (%)	Band size (bp)	na	ne	I	PIC	Ho	He
2-5FR	100.00	240-270	3.000	2.752	1.055	0.564	0.000	0.656
3-2FR	82.35	220-260	4.000	2.361	1.089	0.534	0.429	0.598
3-4FR	100.00	170-240	5.000	1.656	0.831	0.374	0.059	0.408
3-9FR	100.00	220-270	5.000	4.099	1.491	0.717	0.706	0.779
4-1FR	100.00	190-250	7.000	3.753	1.557	0.696	0.294	0.756

4-3FR	100.00	370-450	3.000	1.566	0.656	0.327	0.375	0.373
Average			4.500	2.689	1.113	0.535	0.311	0.595
Standard deviation			1.517	1.055	0.356	0.161	0.259	0.172

na: Observed number of alleles, ne: Effective number of alleles, I: Shannon's Information index, PIC: Polymorphism information content, Ho: Observed heterozygosity, He: Expected heterozygosity.

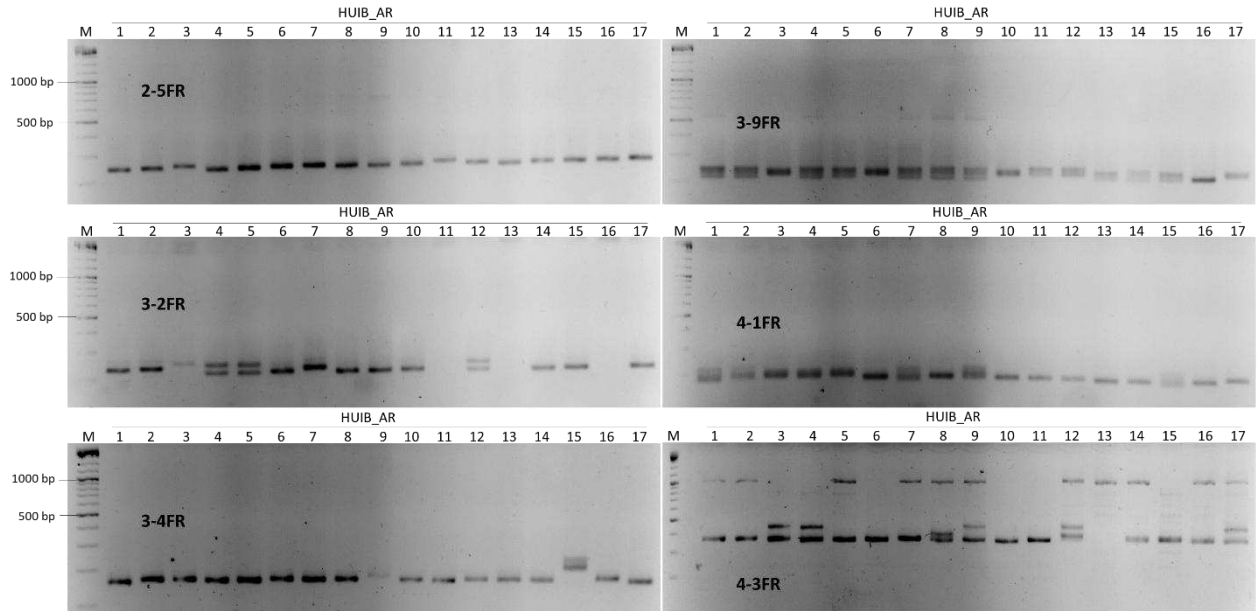


Fig. 5 Electrophoresis results showing PCR products obtained using six pairs of SSR primers. M: GeneRuler 1 kb DNA Ladder.

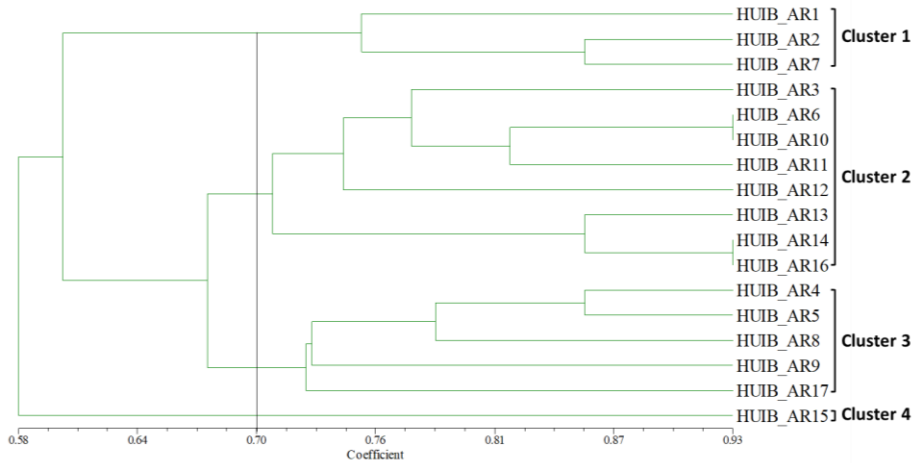


Fig. 6 UPGMA clustering of 17 accessions based on SSR data.

DISCUSSION

Seventeen *Anoectochilus* accessions were investigated and collected in Bach Ma National Park, Vietnam, starting in 2024 (Ho et al. 2025b). Nevertheless, information on micro-morphological and molecular characteristics was lacking for these accessions. This study showed that the morphological characteristics of accessions were similar to previous descriptions of *Anoectochilus roxburghii* by Nguyen et al. (2024). Qualitative morphological traits among the accessions were quite similar. Meanwhile, quantitative traits differed. This was mainly due to differences in growth ability between them. Specifically, HUIB_AR5, HUIB_AR6, HUIB_AR8, HUIB_AR9, and HUIB_AR13 exhibited weak to moderate growth, resulting in lower stem, node, and leaf sizes compared to others. Quantitative traits correlated with each other. Among them, changes in the number of microcellular layers caused changes in the size of the stem, stem nodes, leaves, and petioles. However, floral characteristics were lacking to accurately identify *Anoectochilus roxburghii* based on morphology (Bhattacharjee 2013). To address this limitation, DNA barcoding was used.

DNA barcoding is a tool for species identification using brief, standardized DNA segments. It became a scientific advance during the last 10 years (Nair et al. 2024). Based on the sequencing results of the *ITS*, *rbcL*, and *psbA-trnH* regions, and referencing them against GenBank data, all 17 collected accessions belonged to *Anoectochilus roxburghii*. Furthermore, *ITS* sequencing proved to be the superior method for identifying *Anoectochilus roxburghii* when compared with *rbcL* and *psbA-trnH*. This potential of *ITS* has been previously demonstrated in studies by Thinh et al. (2020) and Lv et al. (2015). In contrast, rbcL was completely conserved. *psbA-trnH* has a high level of species discrimination (Letsiou et al. 2024). Eight nucleotide differences in the *psbA-trnH* region were due to differences in the number of repeats of the TTAGTATA sequence. However, they did not produce polymorphic sites, mutations, recombination events, or haplotype

polymorphisms. Overall, the S, Eta, π, k, h, and Hd values in all three DNA barcode sequences and their combinations were very low. This indicates high genetic homogeneity in these DNA barcode sequences.

Simple sequence repeats (SSRs) or microsatellites have been increasingly used in fingerprinting, genetic diversity studies and population structure analysis of medicinal plants because of their co-dominant and highly polymorphic nature (Bhattarai 2021). Six SSR primers used in this study were shown to be effective in assessing genetic polymorphism among 17 accessions of the same species, *Anoectochilus roxburghii*. Specifically, the UPGMA tree divided this population into four clusters with similarity coefficients ranging over a very large range (0.39-0.93). In addition, HUIB_AR15 was found to be the most distinct based on SSR data. The na, Ho, and He values of the primers were quite high, similar to primers used in Lu's (2022) study. When summarising the characteristics of a locus, the expected heterozygosity (He) is often cited rather than the observed heterozygosity (Ho). Locuses with He values of 0.5 or less are generally not useful for large-scale kinship analysis (Kalinowski et al. 2007). Furthermore, Botstein et al. (1980) showed that PIC $\geq$0.5 indicates high polymorphism information, 0.5 > PIC $\geq$0.25 is medium information, and PIC <0.25 is low information. Therefore, based on He and PIC values greater than 0.5, 2-5FR, 3-2FR, 3-9FR, and 4-1FR are the most promising primers for assessing polymorphism and analysing kinship within a population. The contrast between barcode homogeneity and SSR diversity highlighted distinct evolutionary dynamics within this species.

Anoectochilus roxburghii is a rare herb species. Therefore, studying its morphological and genetic characteristics is of great importance for its conservation and development. Morphological analysis remains standard for identifying species, especially in field surveys where rapid identification is required (Trail 2021). Molecular markers, such as SSR, monitor genetic stability and assess hybridisation/introgression risks, which are essential for breeding programs. Combining both methods provides a more comprehensive view of the evolutionary process and the actual status of a species. In this study, we provided external morphological and internal microscopic characteristics to serve as a basis for rapid identification of *Anoectochilus roxburghii* in Bach Ma National Park, Vietnam. Furthermore, published DNA barcode sequences can serve as a basis for remote population monitoring and identification of illegally traded specimens. Additionally, SSR results showed the presence of several genetic variations in the *Anoectochilus* population, which may indicate the intra-population evolution. According to Zhu et al. (2023), these can provide new ideas for the protection of core germplasms, variety identification and molecular marker-assisted breeding of medicinal plants. Moreover, due to the small number of samples collected, this study has not yet been able to assess the association between SSR markers and differences in morphological characteristics. Therefore, further studies may gather additional accessions and data to assess this association.

Author contributions Conceptualization, N.T.H.H.; methodology, N.T.H.H. and H.T.H.T.; validation, N.T.H.H.; formal analysis, N.T.H.H.; investigation, N.T.H.H.; data curation, N.T.H.H.; writing-original draft preparation, N.T.H.H. and H.T.H.T.; writing-review and editing, N.T.H.H. and H.N.H; visualization, N.T.H.H.; supervision, N.T.H.H. All authors have read and agreed to the published version of the manuscript.

Acknowledgements The authors acknowledge the funding of the Department of Science and Technology of Hue City, Vietnam (Grant No. TTH.2021-KC.31) and the partial support of Hue University under the Core Research Program (Grant No. NCTB.DHH.2024.03). Additionally, we thank B.S. Nhan Van Nguyen from the University of Danang - University of Science and Technology, Danang city, Vietnam, for supporting experiments.

Funding This research was funded by the Department of Science and Technology of Hue City, Vietnam, Grant No. TTH.2021-KC.31, and partially supported by Hue University under the Core Research Program, Grant No. NCTB.DHH.2024.03.

Data Availability The datasets generated and analysed during the current study are available from the corresponding author on reasonable request.

Declarations

Competing Interests The author declares no competing interests.

ORCID

Nhi Thi Hoang Ho https://orcid.org/0000-0001-5197-740X
Han Ngoc Ho https://orcid.org/0000-0002-4583-1807
Hai Thi Hong Truong https://orcid.org/0000-0002-6591-5485

REFERENCES

Barwant MM, Darandale A, Jadhav V, Shrivastava R (2024) Manual for Studying of Morphology and Anatomy of Angiospermic Plants. Journal of Biology 6(1). https://doi.org/10.1042/JB.6.1.0012

Bhattacharjee A (2013) A note on the identity of *Anoectochilus* roxburghii (Orchidaceae). The MIOS Journal 14(6):8-13.

Bhattarai G, Shi A, Kandel DR, Solís-Gracia N, Silva JA, Avila CA (2021) Genome-wide simple sequence repeats (SSR) markers discovered from whole-genome sequence comparisons of multiple spinach accessions. Scientific Reports 11, 9999. https://doi.org/10.1038/s41598-021-89473-0

Botstein D, White RL, Skolnick M, Davis R (1980). Construction of a genetic linkage map in man using restriction fragment length polymorphisms. The American Journal of Human Genetics 32(3):314-331.
Ding Y, Zhang J, Lu Y, Lin E, Lou L, Tong Z (2015). Development of EST-SSR markers and analysis of genetic diversity in natural populations of endemic and endangered plant *Phoebe chekiangensis*. Biochemical Systematics and Ecology 63:183-189. https://doi.org/10.1016/j.bse.2015.10.008
Gao C, Zhang F, Zhang J, Guo S, Shao H (2009) Identification of *Anoectochilus* based on rDNA ITS sequences alignment and SELDI-TOF-MS. International Journal of Biological Sciences 5(7):727-735. https://doi.org/10.7150/ijbs.5.727
Ho NTH, Ho HN, Nguyen TQD, Truong HTH (2025a) Genetic diversity of *Anoectochilus roxburghii* in Hue city, Vietnam, based on RAPD markers. Hue University Journal of Science: Agriculture and Rural Development 134(3D). https://doi.org/10.26459/hueunijard.v134i3D.7774
Ho NTH, Tran AT, Le NTN, Ho HN, Truong HTH (2025b). Distribution of *Anoectochilus roxburghii* (Wall.) Lindl in Bach Ma National Park of central Vietnam. Bangladesh Journal of Botany 54(2):253-260. https://doi.org/10.3329/bjb.v54i2.82289
Ho VT, Tran TKP, Vu TTT, Widiarsih S (2021). Comparison of matK and rbcL DNA barcodes for genetic classification of jewel orchid accessions in Vietnam. Journal of Genetic Engineering and Biotechnology 19(1). https://doi.org/10.1186/s43141-021-00188-1
Hou Y, Wu L, Jiang F, Fan X, Luo D, Ai X, Wang J, Yang M (2025) Predicting the potential distribution and climatic response of the endangered medicinal and edible species, *Anoectochilus roxburghii*, using an optimized MaxEnt model. Scientific Reports 15, 40978. https://doi.org/10.1038/s41598-025-24730-0
Hu SY, Hu HY, Liu X, Chen SL (2019) DNA barcoding and rapid identification of the precious herb Herba Anoectochili. Chinese Journal of Natural Medicines 17(10):0738-0745. https://doi.org/10.1016/S1875-5364(19)30090-1
Kalinowski ST, Taper ML, Marshall TC (2007) Revising how the computer program CERVUS accommodates genotyping error increases success in paternity assignment. Molecular ecology 16(5):1099-1106. https://doi.org/10.1111/j.1365-294X.2007.03089.x
Kumar S, Stecher G, Suleski M, Sanderford M, Sharma S, Tamura K (2024) MEGA12: Molecular Evolutionary Genetic Analysis Version 12 for Adaptive and Green Computing. Molecular Biology and Evolution 41(12). https://doi.org/10.1093/molbev/msae263
Letsiou S, Madesis P, Vasdekis E, Montemurro C, Grigoriou ME, Skavdis G, Moussis V, Koutelidakis AE, Tzakos AG (2024) DNA Barcoding as a Plant Identification Method. Applied Sciences 14(4), 1415. https://doi.org/10.3390/app14041415
Lu S (2022) Transcriptome analysis and development of EST-SSR markers in *Anoectochilus emeiensis* (Orchidaceae). PLoS ONE 17(12), e0278551. https://doi.org/10.1371/journal.pone.0278551
Lv T, Teng R, Shao Q, Wang H, Zhang W, Li M, Zhang L (2015) DNA barcodes for the identification of *Anoectochilus roxburghii* and its adulterants. Planta 242(5):1167-1174. https://doi.org/10.1007/s00425-015-2353-x
Nair VD, Aseema P, Saini KC (2024) DNA barcoding: An effective molecular tool for species identification, molecular authenti-cation and phylogeny studies in plant science research. Plant Science Today 11(4):204-218. https://doi.org/10.14719/pst.3183
Nguyen KD, Nguyen VT, Nguyen VD, To TN, Bui TX (2024) Morphological, anatomical characteristics of *Anoectochilus roxburghii* (Wall.) Lindl. Species in Tam Dao district, Vinh Phuc province. Science and Technology Journal of Agriculture and Rural Development, Vietnam. https://tapchikhoahoc.nnmt.net.vn/vjae/article/view/10/pdf
Nguyen TNS, Tran DTNH, Thai TMP, Le MQ, Tran MH, Le THV (2022) Study on the morphological characteristics and preliminary analysis of the chemical compostion of *Anoectochilus formasanus* Hayata. Dong A University Journal of Science 1(1):39-48. https://js.donga.edu.vn/index.php/daujs/article/view/5
Rozas J, Ferrer-Mata A, Sánchez-DelBarrio JC, Guirao-Rico S, Librado P, Ramos-Onsins SE, Sánchez-Gracia A (2017) DnaSP 6: DNA Sequence Polymorphism Analysis of Large Data Sets. Molecular Biology and Evolution 34(12):3299-3302. https://doi.org/10.1093/molbev/msx248
Safhi FA, Alshamrani SM, Bogmaza AFM, El-Moneim DA (2023) DNA Barcoding of Wild Plants with Potential Medicinal Properties from Faifa Mountains in Saudi Arabia. Genes 14, 469. https://doi.org/10.3390/genes14020469
Sontikun Y, Somwong B, Kanjanasopa D, Thitithanakul S, Suraninpong P (2025) Development of SSR markers and assessment of genetic diversity in native *Nepenthes* spp. in southern Thailand. Ornamental Horticulture 31, e312847. https://doi.org/10.1590/2447-536X.v31.e312847
Su Y, Fu J, Xie H, Huang Z, Li Y, Luo Y, Zhou X, Li Y, Li J, Sun Y, Liu Y (2025) SSR markers development and their application in genetic diversity of burdock (*Arctium lappa* L.) germplasm. BMC Plant Biology 25(196). https://doi.org/10.1186/s12870-025-06203-8
Thinh BB, Chac LD, Thu LTM (2020) Application of internal transcribed spacer (ITS) sequences for identifying *Anoectochilus setaceus* Blume in Thanh Hoa, Vietnam. Proceedings on applied botany, genetics and breeding 181(2):108-116. https://doi.org/10.30901/2227-8834-2020-2-108-116
Trail PW (2021) Morphological analysis: A powerful tool in wildlife forensic biology. Forensic Science International: Animals and Environments 1, 100025. https://doi.org/10.1016/j.fsiae.2021.100025
Tran TKP, Pham MH, Trinh TH, Widiarsih S, Ho VT (2022) Investigation of the genetic diversity of jewel orchid in Vietnam using RAPD and ISSR markers. Biodiversitas Journal of Biological Diversity 23(9):4816-4825. https://doi.org/10.13057/biodiv/d230950
Truong HTH, Ho NTH, Ho HN, Hoang TX (2025) Micro-morphological and molecular characterization of *Centella asiatica* germplasm collected in Vietnam and Laos. Research Journal of Biotechnology 20(8). https://doi.org/10.25303/208rjbt0108
Wang H, Chen X, Yan X, Xu Z, Shao Q, Wu X, Wang H (2022) Induction, proliferation, regeneration and kinsenoside and flavonoid content analysis of the *Anoectochilus roxburghii* (Wall.) Lindl protocorm-like body. Plants 11(19), 2465.
Wang H, Li L, Ye J, Jiang H, Wang Q, Liu Z, Zheng B, Bai Y, Li S (2025) Integrated phenotypic, DNA barcoding, chemotypic, metabolomic, and transcriptomic analyses for quality assessment of *Anoectochilus roxburghii* and identification of key metabolites and enzyme genes in kinsenoside biosynthesis and leaf non-green coloration. Industrial Crops & Products 235, 121770. https://doi.org/10.1016/j.indcrop.2025.121770
Woodruff DS (2001) Populations, Species, and Conservation Genetics. Encyclopedia of Biodiversity. https://doi.org/10.1016/B0-12-226865-2/00355-2
Ye S, Shao Q, Xu M, Li S, Wu M, Tan X, Su L (2017) Effects of Light Quality on Morphology, Enzyme Activities, and Bioactive Compound Contents in *Anoectochilus roxburghii*. Frontiers in Plant Science 8:857. https://doi.org/10.3389/fpls.2017.00857
Ye S, Wang Z, Shen J, Shao Q, Fang H, Zheng B, Younis A (2019) Sensory qualities, aroma components, and bioactive compounds of *Anoectochilus roxburghii* (Wall.) Lindl. as affected by different drying methods. Industrial Crops & Products 134:80-88. https://doi.org/10.1016/j.indcrop.2019.03.063
Zaman W, Ayaz A, Park S (2025) Integrating morphological and molecular data in plant taxonomy. Pakistan Journal of Botany 57(4). http://dx.doi.org/10.30848/PJB2025-4(27)
Zhang W, Chen K, Mei Y, Wang J (2024) De Novo Transcriptome Assembly of *Anoectochilus roxburghii* for Morphological Diversity Assessment and Potential Marker Development. Plants 13, 3262. https://doi.org/10.3390/plants13233262
Zhang FS, Lv YL, Zhao Y, Guo SX (2013) Promoting role of an endophyte on the growth and contents of kinsenosides and flavonoids of *Anoectochilus formosanus* Hayata, a rare and threatened medicinal Orchidaceae plant. Journal of Zhejiang University Science B 14(9):785–792. https://doi.org/10.1631/jzus.B1300056
Zhao Z, Zhang H, Wang P, Yang Y, Sun H, Li J, Chen X, Li J, Ji N, Feng H, Zhao S (2023) Development of SSR molecular markers and genetic diversity analysis of *Clematis acerifolia* from Taihang Mountains. PLoS ONE 18(5), e0285754. https://doi.org/10.1371/journal.pone.0285754
Zhu Y, Ma T, Lin Y, Peng Y, Huang Y, Jiang J (2023) SSR molecular marker developments and genetic diversity analysis of *Zanthoxylum nitidum* (Roxb.) DC. Scientific Reports 13(20767). https://doi.org/10.1038/s41598-023-48022-7
Zou X, Zhang K, Li X, Zhang Y, Chen L, Li H (2025) Current advances on the phytochemistry, pharmacology, quality control and applications of *Anoectochilus roxburghii*. Fronties in Pharmacology 15, 1527341. https://doi.org/10.3389/fphar.2024.1527341